Imperial College London

9 December 2021

Computational Imaging for Art Investigation and for Neuroscience

Pier Luigi Dragotti

Imperial College London

Motivation

- The revolution in sensing, with the emergence of many new sensing and imaging techniques, offers the possibility of gaining unprecedented access to the physical world

- In order to fully exploit these advances, it is necessary to rethink imaging as an integrated sensing and inference model

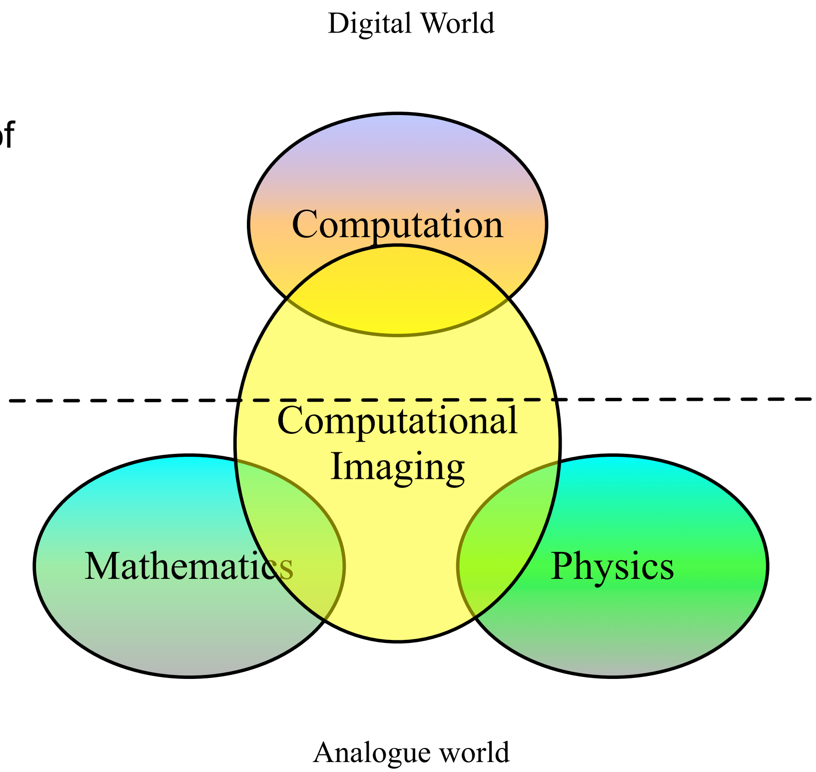

Imperial College London

Outline

In this talk we will cover two research areas where Computational Imaging can have an impact:

Technical Study of Old Masters Paintings

Microscopy and Neuroscience

Imperial College London

Joint work with

Nathan Daly

Su Yan

Catherine Higgitt

Junjie Huang

Pingfan Song

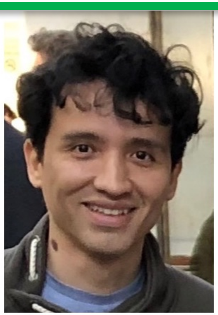

Herman Verinaz

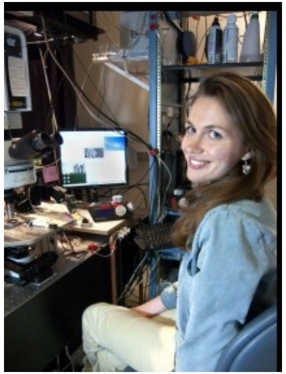

Amanda Foust

Carmel Howe

Peter Quicke

Imperial College London

Technical Examination of Paintings

Imperial College London

Structure of a painting

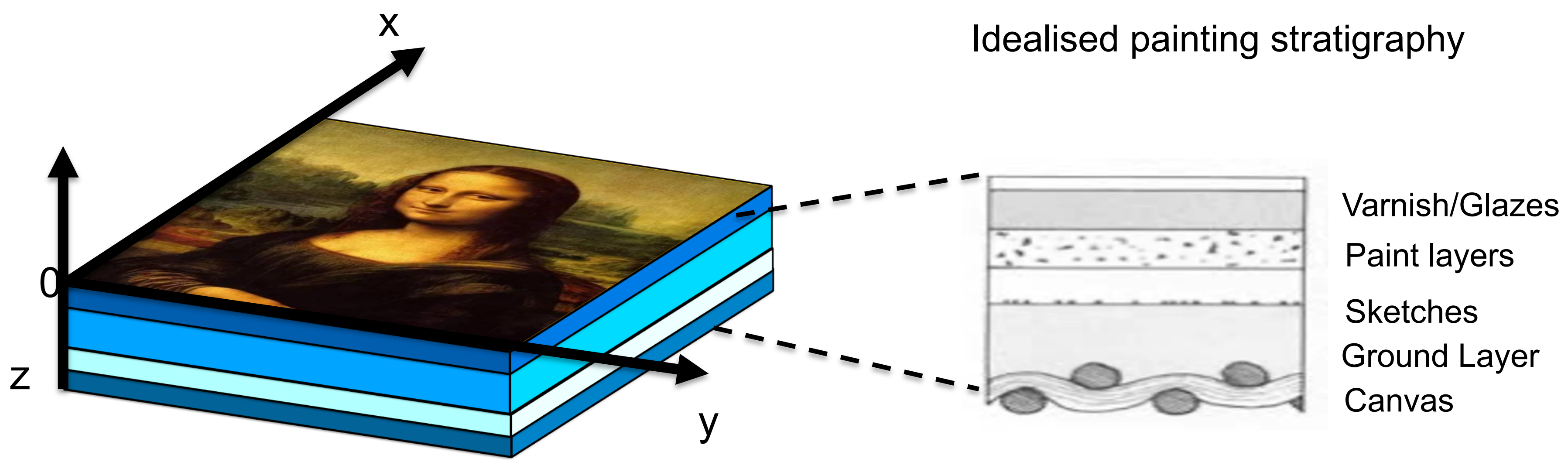

Structure of a painting

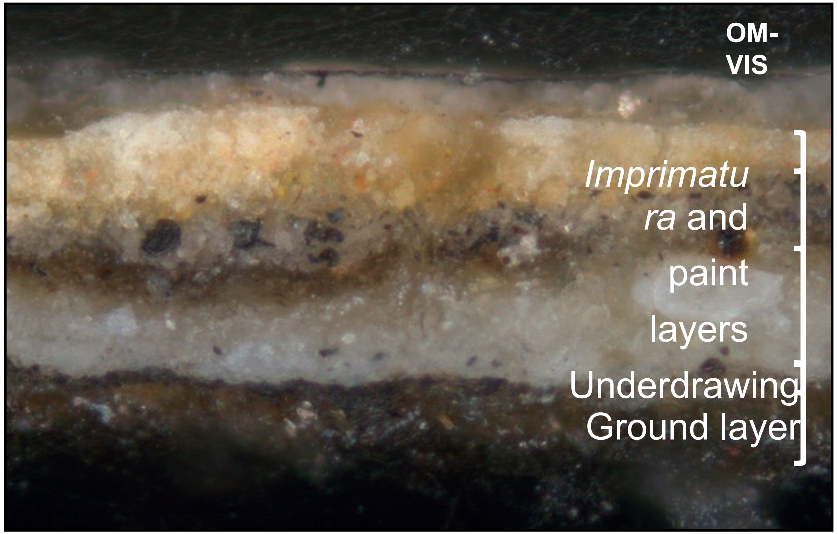

Leonardo, *The Virgin of the Rocks*,
about 1491/2-9 and 1506-8
National Gallery (NG1093)

Imperial College London

Traditional Non-Invasive Imaging Methods

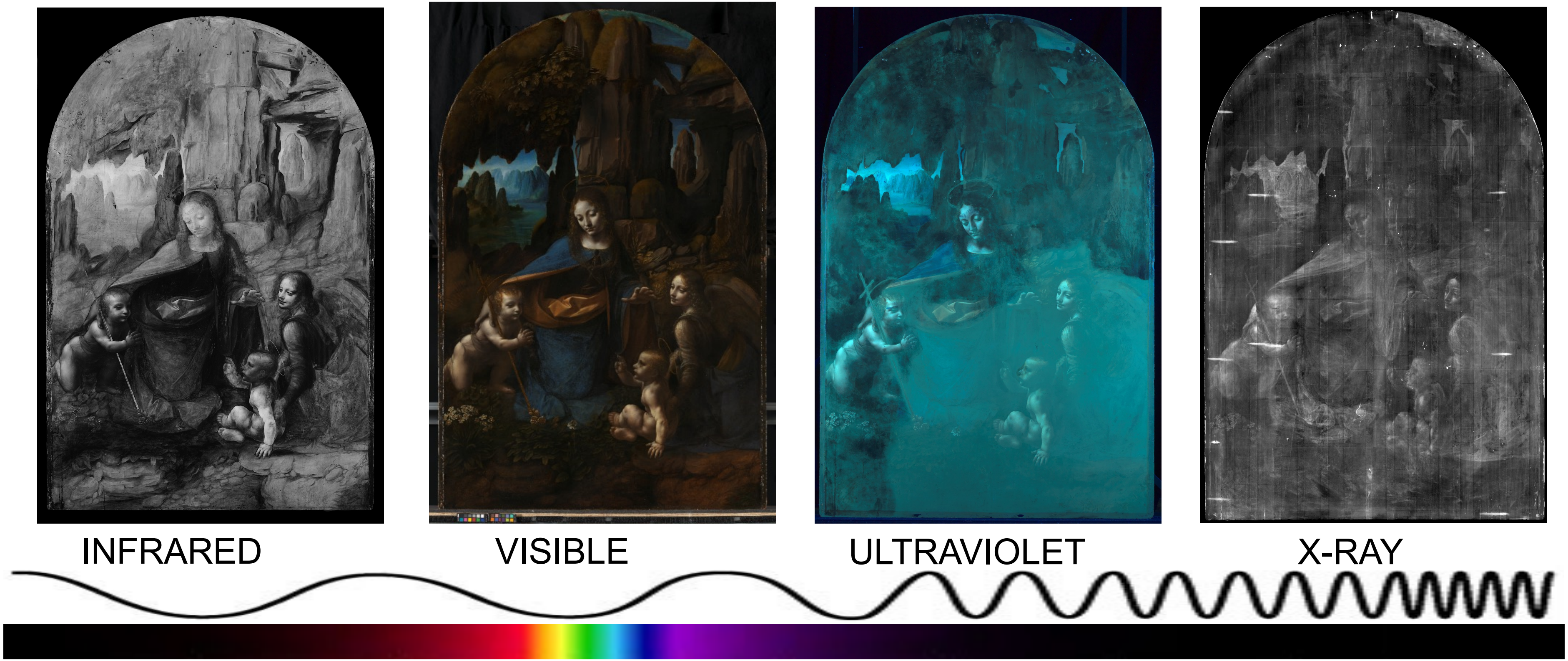

Imperial College London

Macro X-Ray Fluorescence (MA-XRF)

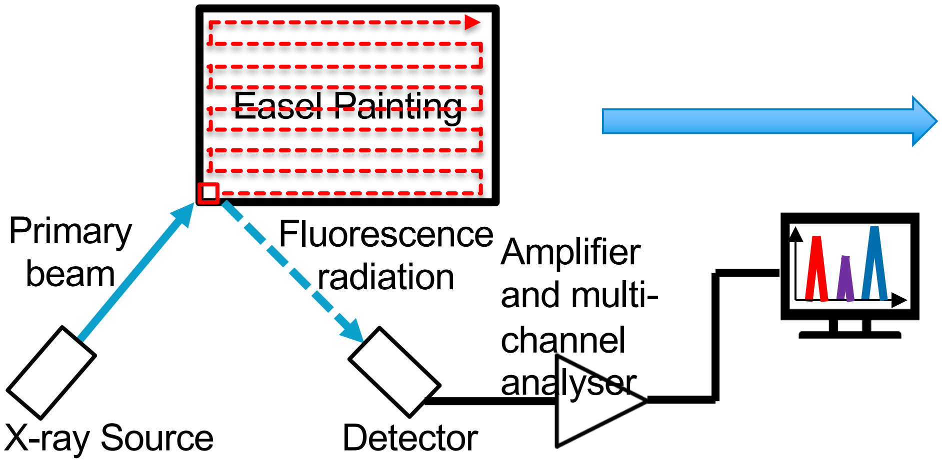

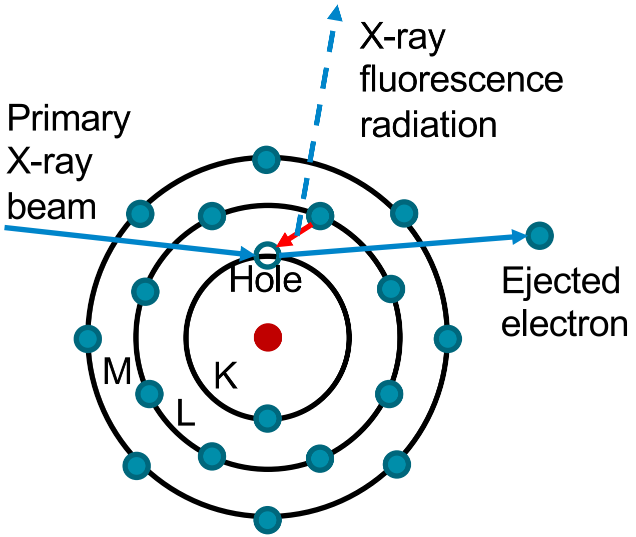

Macro X-Ray Fluorescence (MA-XRF)

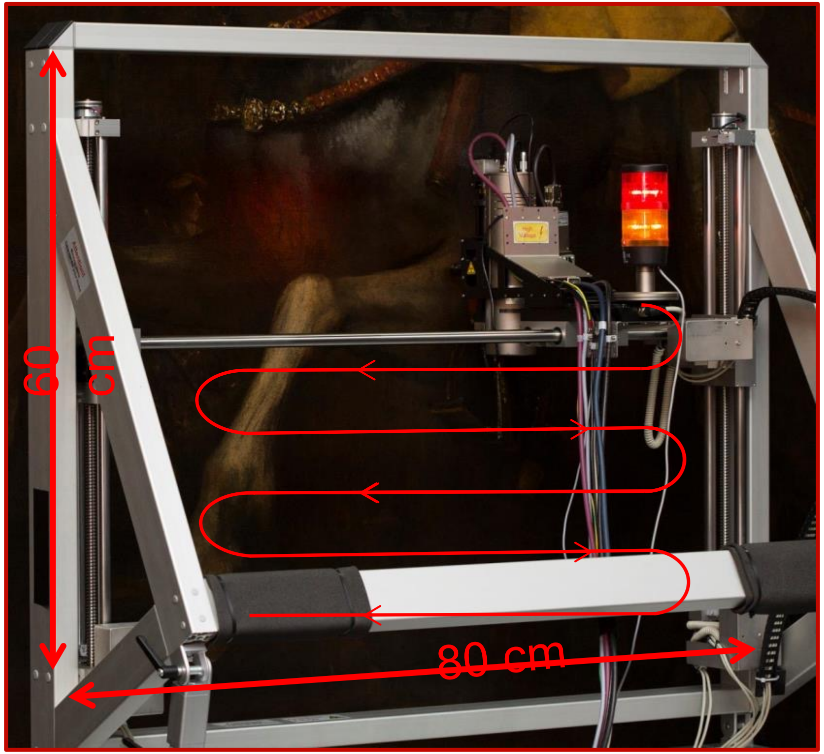

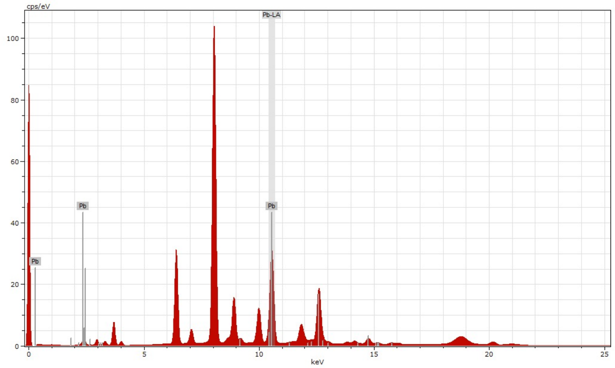

MA-XRF Datacube and Spectrum

- Macro X-ray provides volumetric data and the locations of the pulses in the energy direction are related to the chemical elements present in the painting.
- This potentially allows us to create maps that show the distribution of different chemical elements

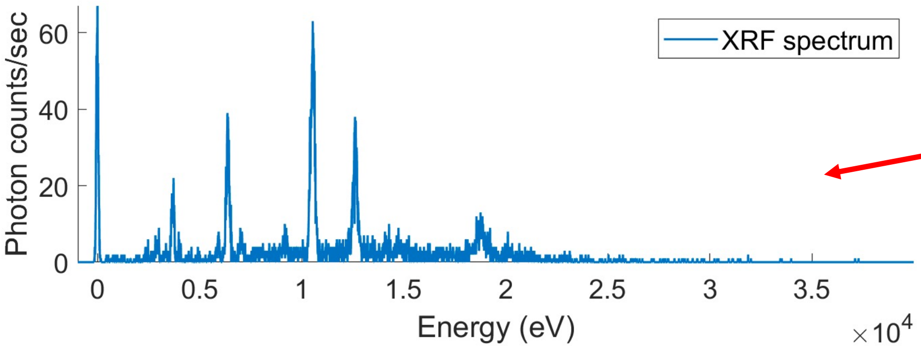

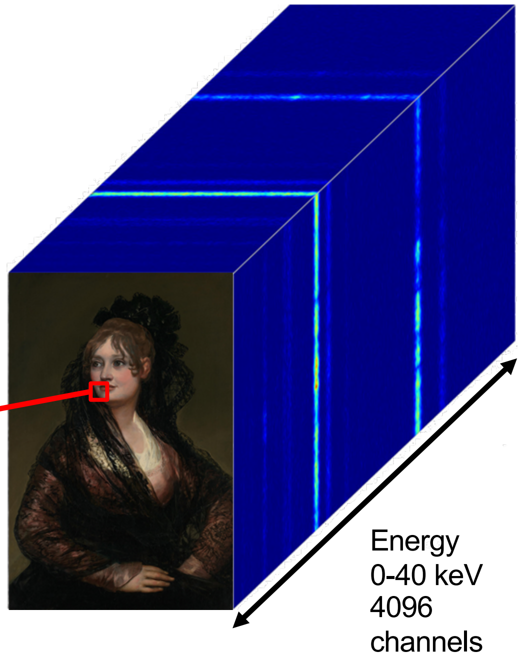

MA-XRF Datacube and Spectrum

Imperial College London

- Macro X-ray provides volumetric data and the locations of the pulses in the energy direction are related to the chemical elements present in the painting.
- This potentially allows us to create maps that show the distribution of different chemical elements

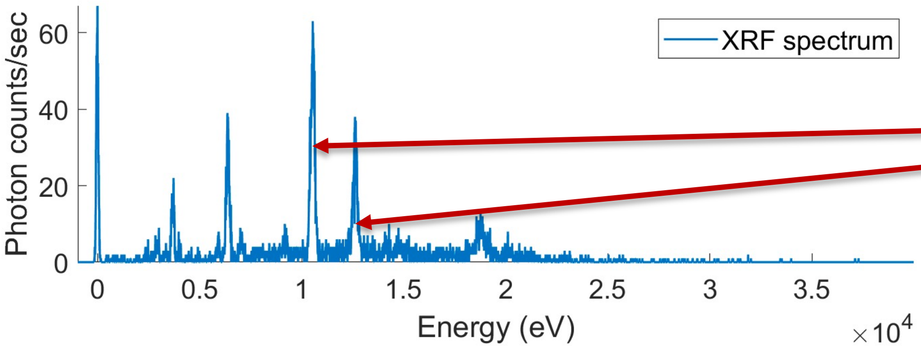

Element	Atomic No.	*K* series				*L* series						*M* series
		K_α group		K_β group		L_l group	L_α group		L_β group		L_γ group	M_α group
		$K_{\alpha 1}$	$K_{\alpha 2}$	$K_{\beta 1}$	$K_{\beta 2}$	L_l	$L_{\alpha 1}$	$L_{\alpha 2}$	$L_{\beta 1}$	$L_{\beta 2}$	$L_{\gamma 1}$	$M_{\alpha 1}$
Al	13	1487	/	1557	/	/	/	/	/	/	/	/
Si	14	1740	/	1836	/	/	/	/	/	/	/	/
P	15	2014	/	2139	/	/	/	/	/	/	/	/
S	16	2307	/	2464	/	/	/	/	/	/	/	/
Cl	17	2622	/	2816	/	/	/	/	/	/	/	/
Ar	18	2957	/	3191	/	/	/	/	/	/	/	/
K	19	3313	/	3590	/	/	/	/	/	/	/	/
Ca	20	3690	/	4013	/	/	/	/	/	/	/	/
Ti	22	4509	/	4932	/	/	/	/	/	/	/	/
V	23	4950	/	5427	/	/	/	/	/	/	/	/
Cr	24	5412	/	5947	/	/	/	/	/	/	/	/
Mn	25	5895	/	6490	/	/	/	/	/	/	/	/
Fe	26	6400	/	7058	/	/	/	/	/	/	/	/
Co	27	6925	/	7649	/	/	/	/	/	/	/	/
Ni	28	7472	/	8265	/	/	/	/	/	/	/	/
Cu	29	8041	/	8905	/	/	/	/	/	/	/	/
Zn	30	8631	/	9572	/	/	/	/	/	/	/	/
As	33	10544	10508	11726	11864	/	/	/	/	/	/	/
Br	35	11924	11878	13291	13470	/	/	/	/	/	/	/
Sr	38	14165	14098	15836	16085	1582	1806	/	1872	/	/	/
Rh	45	20216	20074	22724	23173	2377	2695	/	2834	3001	3144	/
Ag	47	22163	21990	24942	25456	2634	2982	/	3151	3348	3520	/
Cd	48	23174	22984	26096	26644	2767	3131	/	3317	3528	3717	/
Sn	50	25271	25044	28486	29109	3045	3441	/	3663	3905	4131	/
Sb	51	26359	26111	29726	30390	3189	3602	/	3844	4101	4348	/
I	53	28612	28317	32295	33042	3485	3934	/	4221	4508	4801	/
Ba	56	32194	31817	36378	37257	3954	4466	4451	4828	5157	5531	/
Au	79	68804	66990	77984	80150	8494	9713	9628	11442	11585	13382	2123
Hg	80	70819	68895	80253	82515	8721	9989	9898	11823	11924	13830	2195
Pb	82	74969	72804	84936	87320	9185	10552	10450	12614	12623	14764	2346
Bi	83	77108	74815	87343	89830	9420	10839	10731	13024	12980	15248	2423

Extraction of Elemental Maps

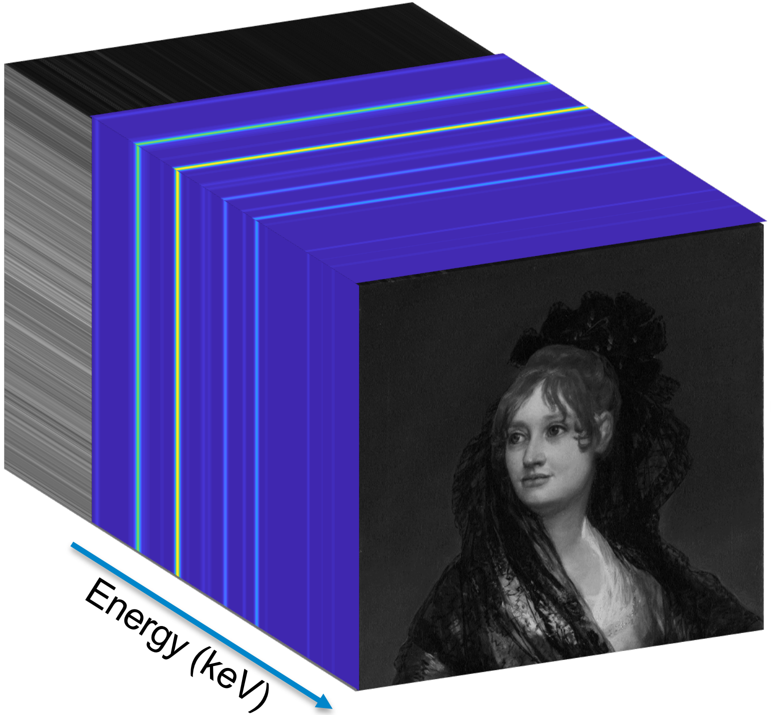

XRF

Deconvolution

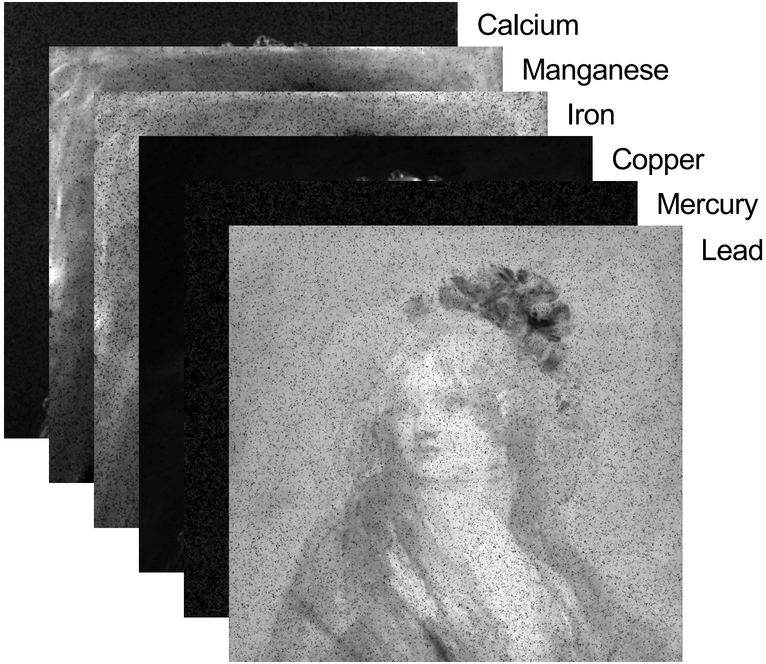

Portrait of Doña Isabel de Porcel, © National Gallery, London (Francisco Goya)

Imperial College London

Challenges in XRF Deconvolution

- Objective:
  - To develop a fully automatic method for processing MA-XRF datacube of the painting which is able to
    - detect and locate the pulses from the MA-XRF spectra
    - identify existing elements and show their distribution maps.
- Challenges:
  - Pulses overlap
  - Important pulses are buried in noise

Imperial College London

Overview of our proposed method

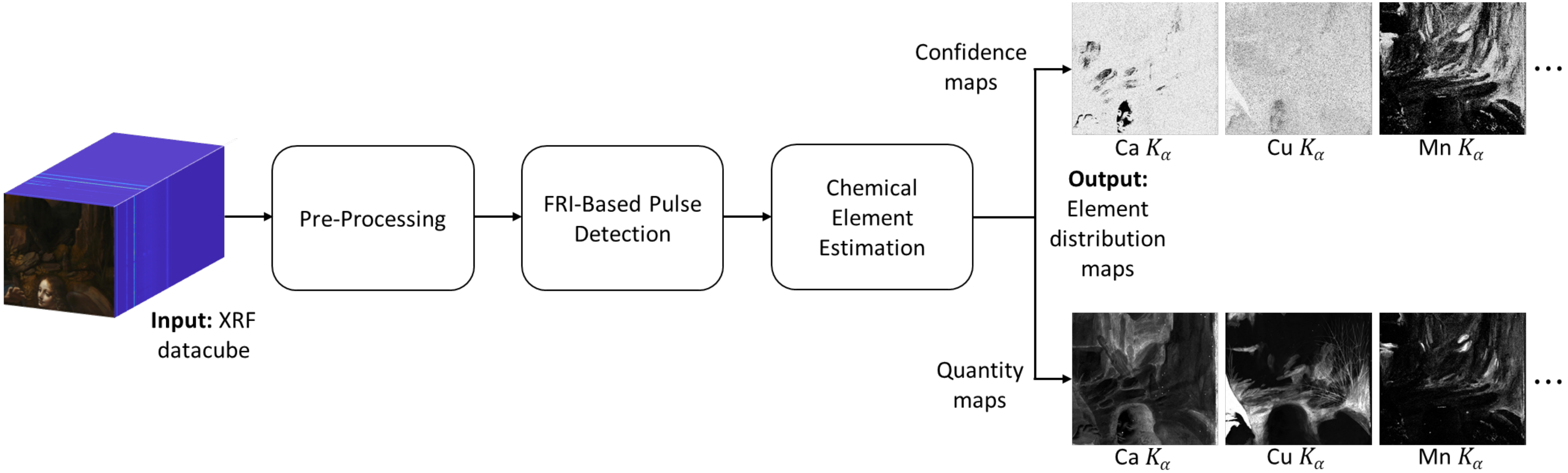

Imperial College London

Proposed Method

- The XRF spectrum can be seen as the sum of K pulses with the same pulse shape $\varphi(\cdot)$ plus the noise ϵ,

$$y[n] = \sum_{k=1}^{K} a_k \varphi[n - t_k] + \epsilon[n],$$

where $n = 0,1,\ldots,l-1$ represents the energy channels.

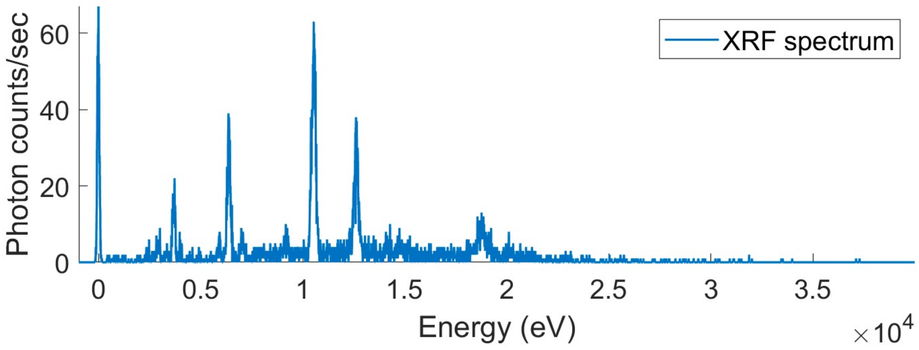

- We need to retrieve amplitudes a_k and locations t_k of the pulses
- The pulse shape is known a-priori
- The amplitude of the pulses must be positive

Imperial College London

Proposed Method

- The key idea is to connect our problem to a method broadly used in engineering and known as Prony's method

$$y[n] \rightarrow s[m] = \sum_{k=1}^{K} b_k u_k^m ,$$

where $b_k = a_k e^{j\omega_0 t_k}$, $u_k = e^{j\lambda t_k}$

- Retrieving the pulse locations u_k and the amplitudes a_k from $s[m]$ is a classical problem first solved by Baron de Prony in 1795.

Proposed Method

- We find coefficients $c_{m,n}$ such that the weighed sum of the pulses $\varphi(t)$ can approximately reproduce complex exponentials:

$$\sum_{n} c_{m,n}\varphi(t-n) \approx e^{j\omega_m t}$$

- For $\omega_m = \omega_0 + m\lambda$, $m = 0,1,\ldots,M$, where M is the number of exponentials we aim to reproduce and ω_0 is arbitrary.

Imperial College London

Proposed Method

$$\sum_n c_{m,n}\varphi(t-n) \approx e^{j\omega_m t}$$

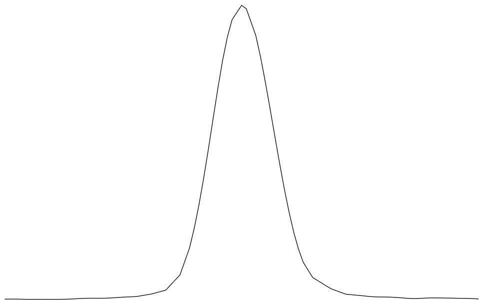

Pulse shape

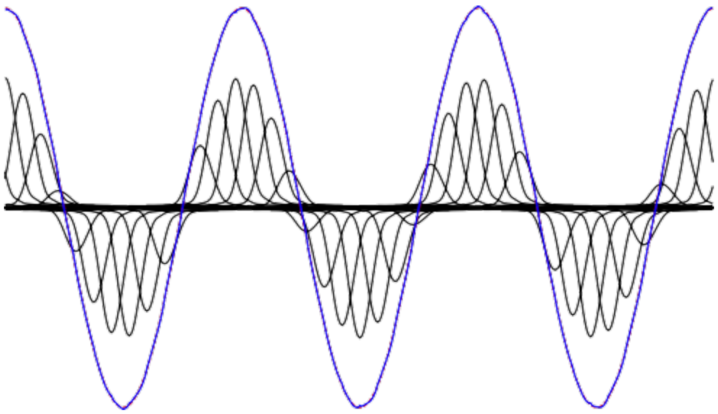

Reproduction of exponentials

Computation of the coefficients $c_{m,n}$

- We want to find coefficients $c_{m,n}$ such that $\sum_n c_{m,n}\varphi(t-n) \approx f_m(t)$ in the least-square sense.
- We need to compute the orthogonal projection of $f_m(t)$ onto $V = \mathrm{span}\{\varphi(t-n)\}_n$
- This means $\langle f_m(t) - \sum_n c_{m,n}\varphi(t-n), \varphi(t-k)\rangle = 0$ (orthogonality principle)
- Leveraging the fact that we are considering uniform shifts of $\varphi(t)$ and that in our case $f_m(t) = e^{j\omega_m t}$, we end-up with an exact expression[1]:

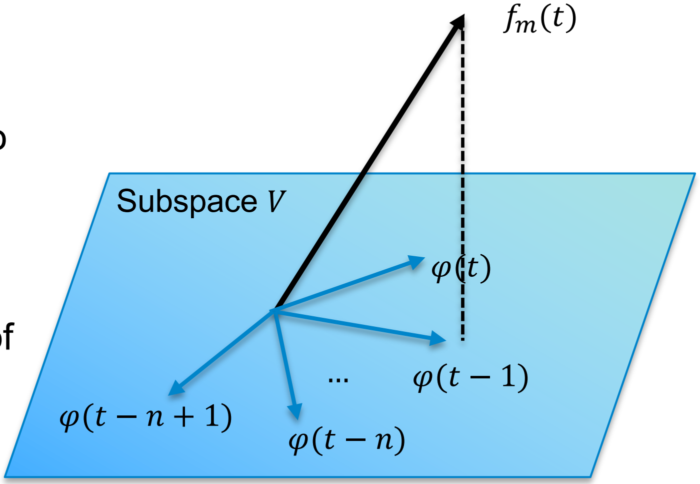

$$c_{m,n} = \frac{\hat{\varphi}(\omega_m)e^{j\omega_m n}}{\widehat{a_\varphi}(e^{j\omega_m})}$$

where $\widehat{a_\varphi}(e^{j\omega_m})$ is the z-transform of $\langle\varphi(t-n), \varphi(t)\rangle$ at $z = e^{j\omega_m}$.

[1] J. Urigüen, T. Blu, and P. Dragotti, "FRI sampling with arbitrary kernels," IEEE Transactions on Signal Processing, vol. 61, no. 21, pp. 5310–5323, 2013.

Imperial College London

Proposed Method

- Moments $s[m]$ are computed as follows:

$$\boxed{s[m]} = \sum_{n=0}^{N-1} c_{m,n} \boxed{y[n]} = \sum_{k=1}^{K} a_k \sum_{n=0}^{N-1} c_{m,n} \varphi[t_k - n]$$

$$\approx \sum_{k=1}^{K} a_k e^{j\omega_m t_k} = \sum_{k=1}^{K} a_k e^{j\omega_0 t_k} \left(e^{j\lambda t_k}\right)^m = \boxed{\sum_{k=1}^{K} b_k u_k^m},$$

where $b_k = a_k e^{j\omega_0 t_k}$, $u_k = e^{j\lambda t_k}$

- The amplitudes a_k and locations t_k can now be retrieved using Prony's method.

Imperial College London

Prony's Method

Assume: $s_m = \sum_{k=1}^{K} b_k u_k^m$ and consider the polynomial:

$$P(x) = \prod_{k=1}^{K}(x - u_k) = x^K + h_1 x^{K-1} + h_2 x^{K-2} + \ldots + h_{K-1}x + h_K.$$

It is easy to verify that

$$s_{n+K} + h_1 s_{n+K-1} + h_2 s_{n+K-2} + \ldots + h_K s_n = \sum_{1\le k\le K} b_k u_k^n P(u_k) = 0.$$

In matrix-vector form for indices n such that $\ell \le n < \ell + K$, we get

$$\begin{bmatrix} s_{\ell+K} & s_{\ell+K-1} & \cdots & s_\ell \\ s_{\ell+K+1} & s_{\ell+K} & \cdots & s_{\ell+1} \\ \vdots & \ddots & \ddots & \vdots \\ s_{\ell+2K-2} & \ddots & \ddots & \vdots \\ s_{\ell+2K-1} & s_{\ell+2K-2} & \cdots & s_{\ell+K-1} \end{bmatrix} \begin{bmatrix} 1 \\ h_1 \\ h_2 \\ \vdots \\ h_K \end{bmatrix} = \mathbf{T}_{K,\ell}\mathbf{h} = \mathbf{0}$$

Prony's Method

The vector of polynomial coefficients $\mathbf{h} = [1, h_1, ..., h_K]^T$ is in the null space of $\mathbf{T}_{K,\ell}$.
Moreover, $\mathbf{T}_{K,\ell}$ has size $K \times (K+1)$ and has full row rank when the u_k's are distinct.
Therefore $\mathbf{h}$ is unique.
Prony's method summary:

1. Given the input s_m, build the Toeplitz matrix $\mathbf{T}_{K,\ell}$ and solve for $\mathbf{h}$. This can be achieved by taking the SVD of $\mathbf{T}_{K,\ell}$.
2. Find the roots of $P(x) = 1 + \sum_{n=1}^{K} h_k x^{K-k}$. These roots are exactly the exponentials $\{u_k\}_{k=1}^{K}$.
3. Given the $\{u_k\}_{k=1}^{K}$, find the corresponding amplitudes $\{b_k\}_{k=1}^{K}$ by solving K linear equations.

Many robust versions of Prony's exist, e.g., Cadzow, matrix pencil etc.

Imperial College London

Estimating the number of pulses

- Prony's method requires the number of pulses K to be known.
- In our case, K, which is related to the elements in the painting, is unknown and need to be estimated *automatically*.
- The algorithm tries different possible Ks and picks the one which leads to a result which is consistent with the physics of the data (all positive pulses) and sufficiently close to the raw data (energy of error $\approx$ energy of background signal).

Imperial College London

Allocating Pulses to Elements

- Once the pulse locations are estimated they are assigned to the chemical elements
- Allocation and confidence depend on the amplitude of the pulse and its distance to the closest emission line

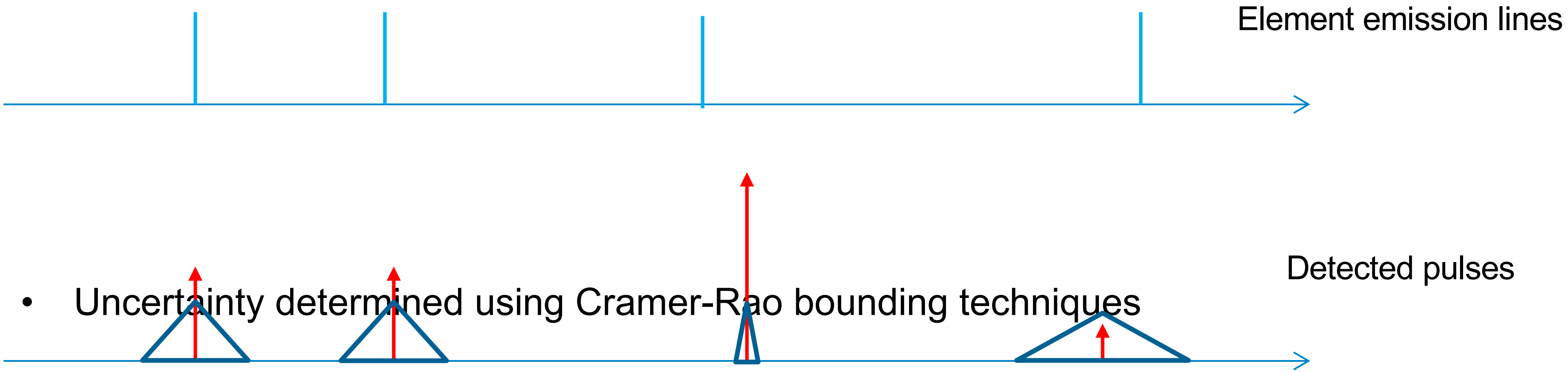

- Uncertainty determined using Cramer-Rao bounding techniques

Imperial College London

Uncertainty factor

- Uncertainty factor depends on the amplitude of the detected pulse a_k, and is proportional to Cramér-Rao Lower Bound of one pulse

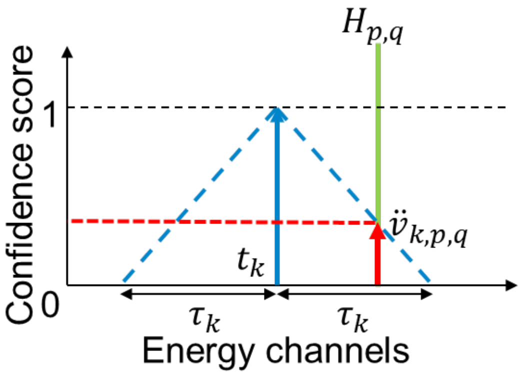

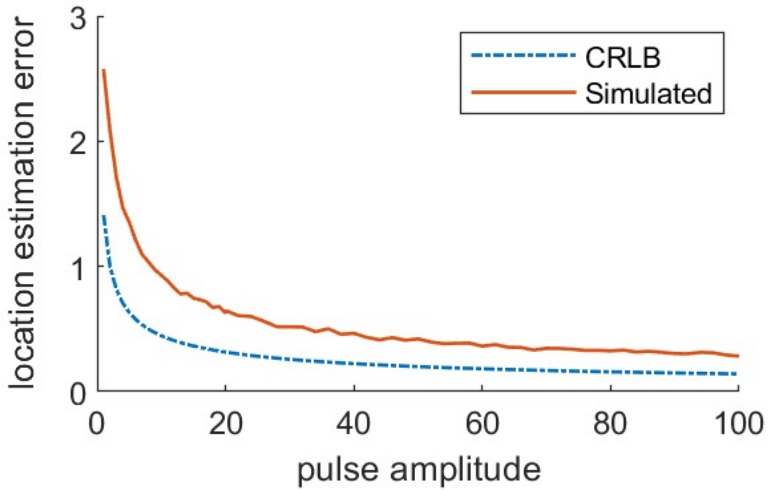

Element Distribution Maps

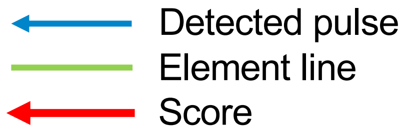

- Confidence score and quantity score

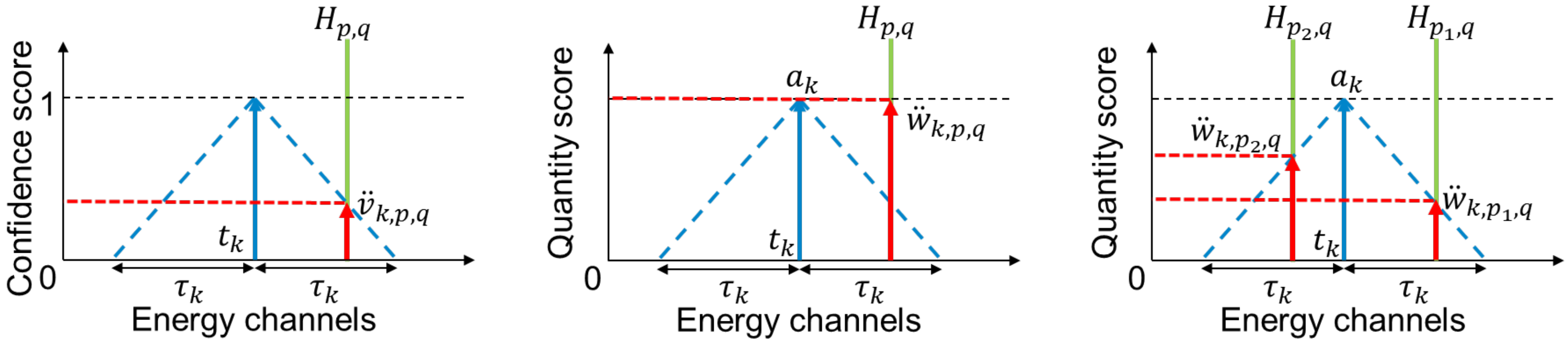

Confidence

Quantity

Imperial College London

Extraction of Elemental Maps

Our XRF

Deconvolution

Algorithm

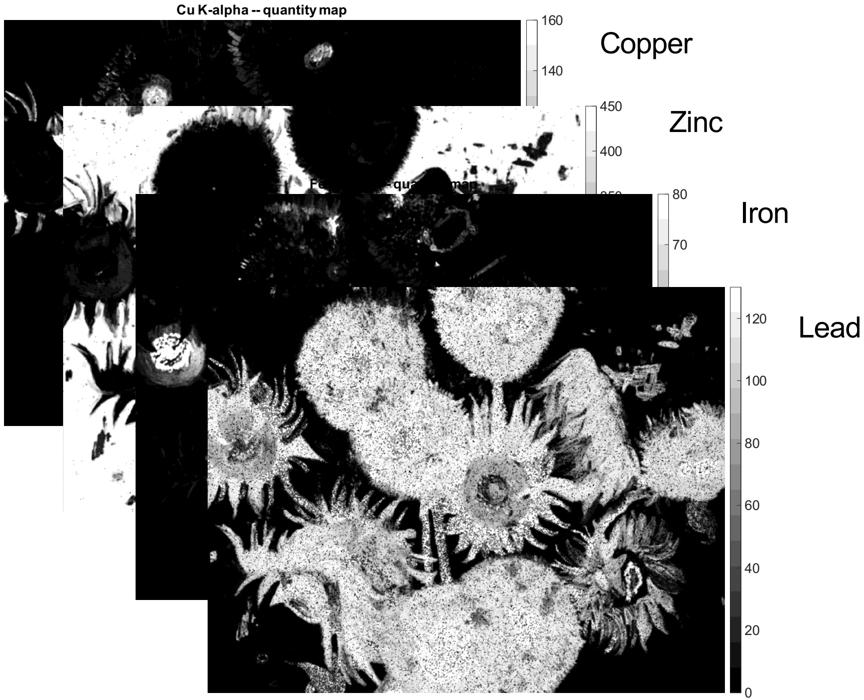

Vincent van Gogh, “Sunflowers (NG3863)”, © The National Gallery, London.

Imperial College London

Results

Leonardo da Vinci's "The Virgin of the Rocks"

Highlighted is the region of an XRF dataset collected on the painting with an M6 Bruker JETSTREAM instrument (30 W Rh anode at 50 kV and 600 μA, 60 mm^2 Si drift detector, and data collected with 350 μm beam and pixel size and 10 ms dwell time).

Leonardo da Vinci, "The Virgin of the Rocks (NG1093)," about 1491/2-9 and 1506-8, oil on poplar, 189.5 x 120 cm, The National Gallery, London.

Imperial College London

Results

Copper (Cu) distribution maps

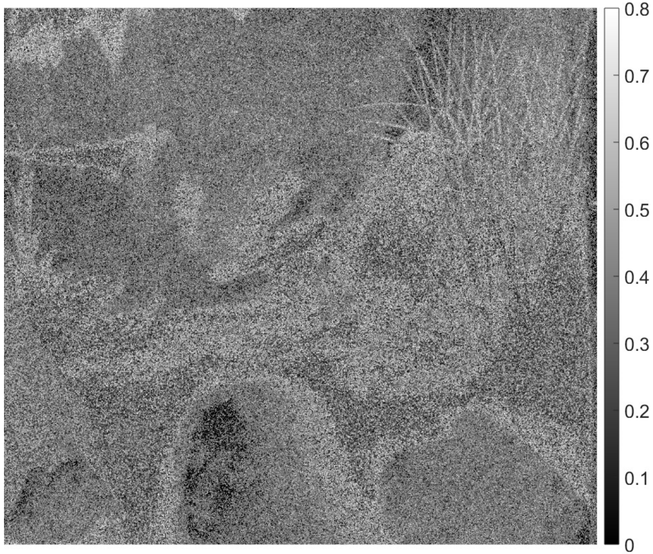

Cu confidence map

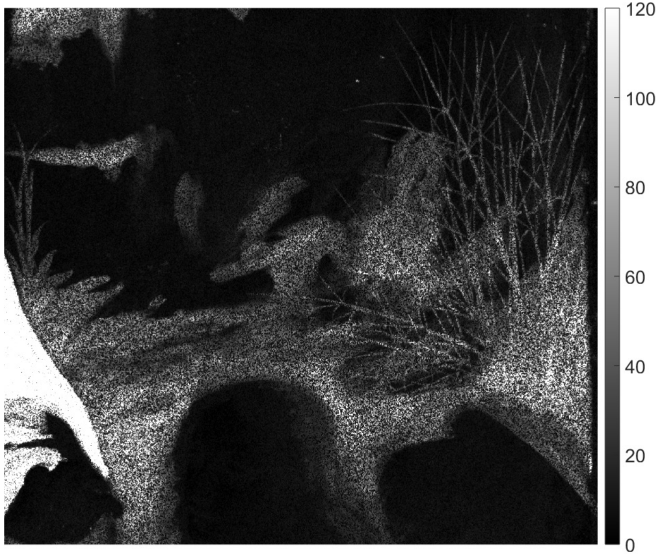

Cu quantity map

Imperial College London

Results

Zinc (Zn) distribution maps

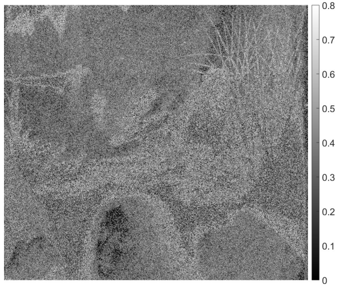

Cu confidence map

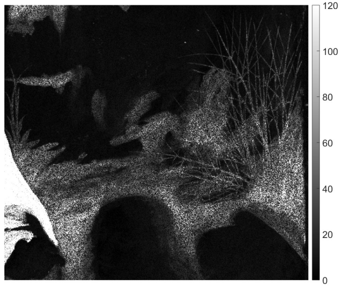

Cu quantity map

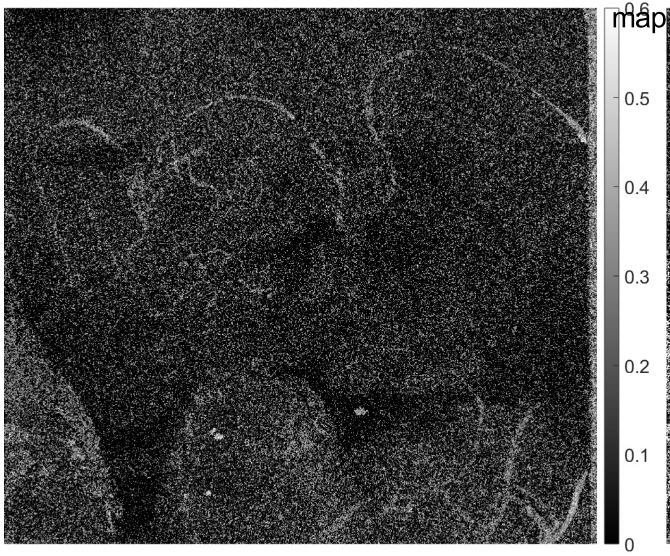

Zn confidence map

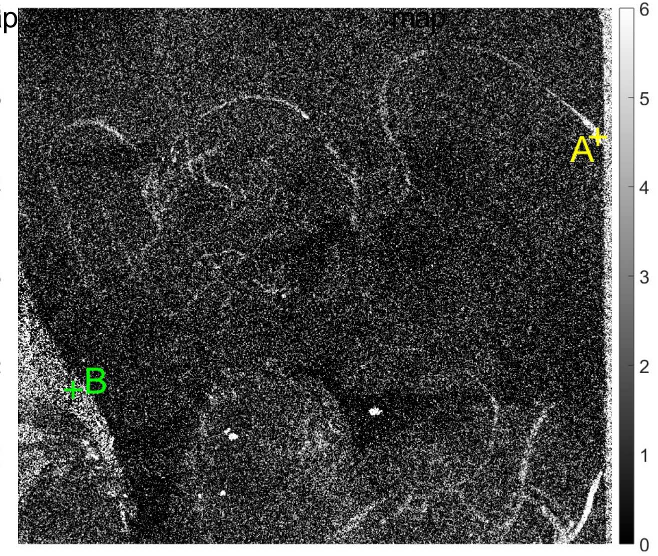

Zn quantity map

Imperial College London

Sample Results

Element	K_α	K_β
Copper (Cu)	901	986
Zinc (Zn)	960	

X-ray characteristic lines

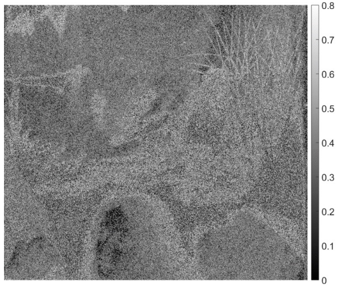

Cu confidence map

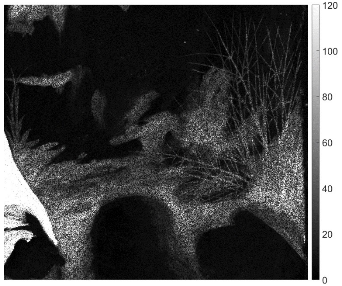

Cu quantity map

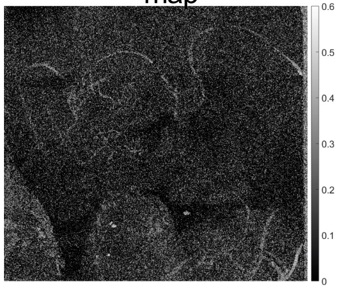

Zn confidence map

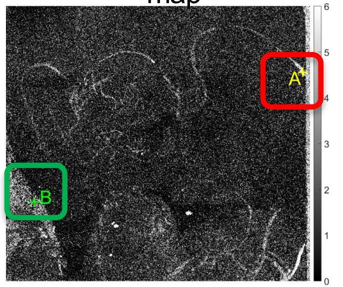

Zn quantity map

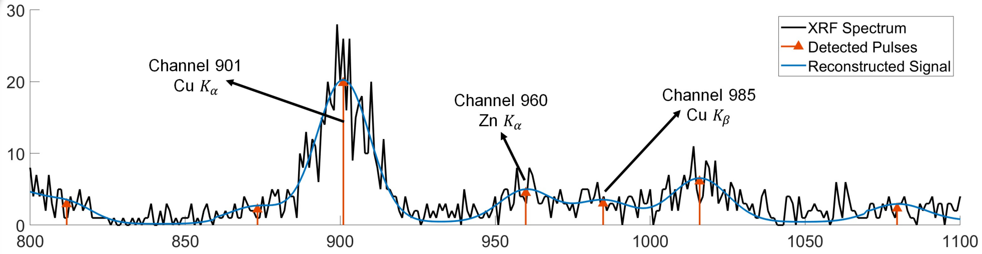

Pulse detection result of **Pixel A** on the angel wing

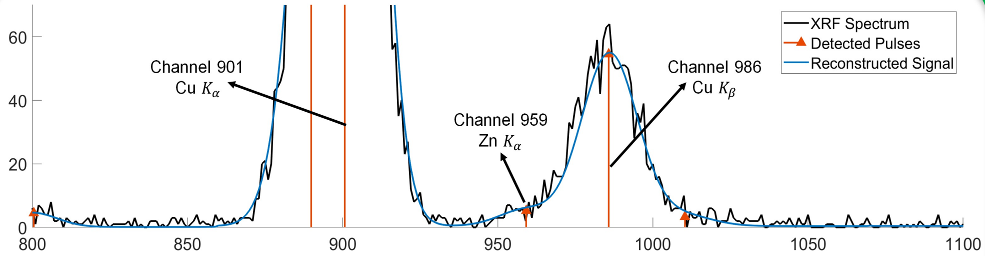

Pulse detection result of **Pixel B** on the drapery

S. Yan, J. Huang, N. Daly, C. Higgitt and P. L. Dragotti, “Revealing Hidden Drawings in Leonardo’s ‘the Virgin of the Rocks’ from Macro X-Ray Fluorescence Scanning Data through Element Line Localisation”, IEEE International Conference on Acoustics, Speech and Signal Processing (ICASSP), May 2020.

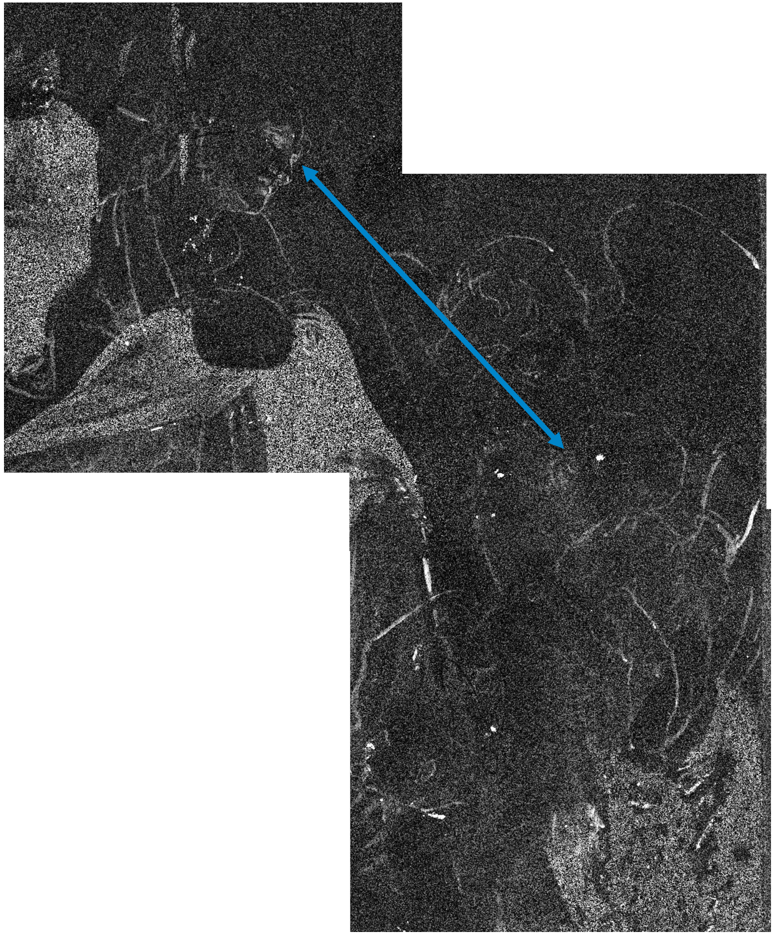

On-going work

Imperial College London

Machine Learning to extract painting underneath (project lead by UCL[1])

(a)

(b)

Francisco de Goya, Dona Isabel de Porcel (NG1473), before 1805. Oil on canvas. (a). RGB image. (b). X-ray image.

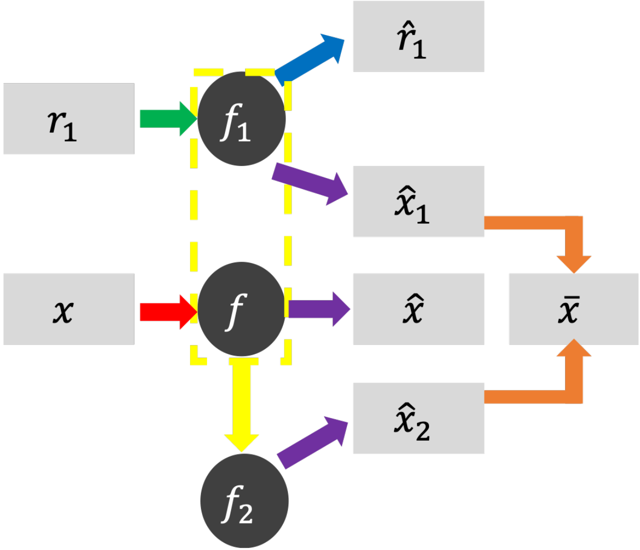

[1]W. Pu, J. Huang, B. Sober, N. Daly, C. Higgitt, P.L. Dragotti, I. Daubechies and M. Rodrigues, "A Learning Based Approach to Separate Mixed X-Ray Images Associated with Artwork with Concealed Designs", EUSIPCO 2021.

On-going work

Machine Learning to extract painting underneath

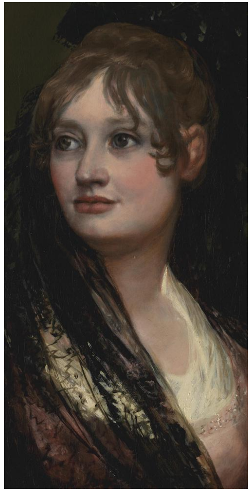

Separation Results

Two-Photon Microscopy for Neuroscience

- Goal of Neuroscience: to study how information is processed in the brain
- Neurons communicate through pulses called Action Potentials (AP)
- Need to measure in-vivo the activity of large populations of neurons at cellular level resolution
- Two-photon microscopy combined with right indicators is the most promising technology to achieve that

Imperial College London

Two-Photon Microscopy

- Fluorescent sensors within tissues
- Highly localized laser excites fluorescence from sensors
- Photons emitted from tissue are collected
- Focal spot sequentially scanned across samples to form image

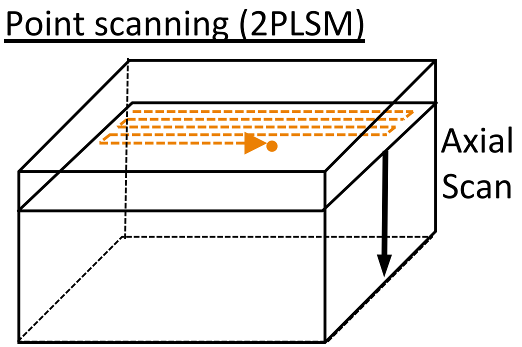

Imperial College London

Two-Photon Microscopy

- Fluorescent sensors within tissues
- Highly localized laser excites fluorescence from sensors
- Photons emitted from tissue are collected
- Focal spot sequentially scanned across samples to form image
- Two-photon microscopes in raster scan modality can go deep in the tissue but are slow

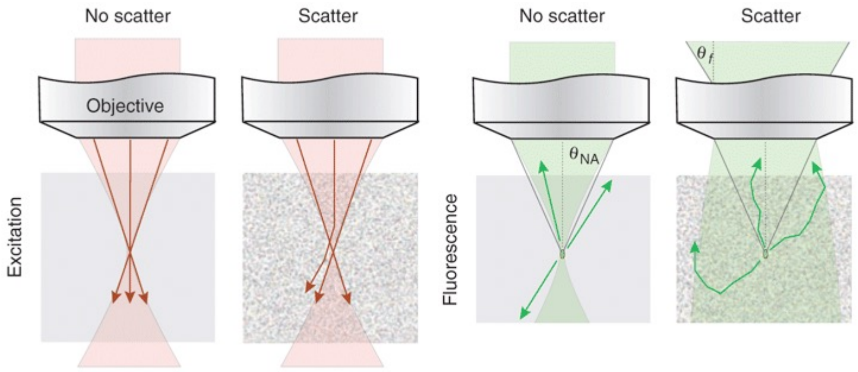

Imperial College London

Two-Photon Microscopy

- In order to speed up acquisition one can change the illumination strategy
- This mitigates the issue but does not fix it

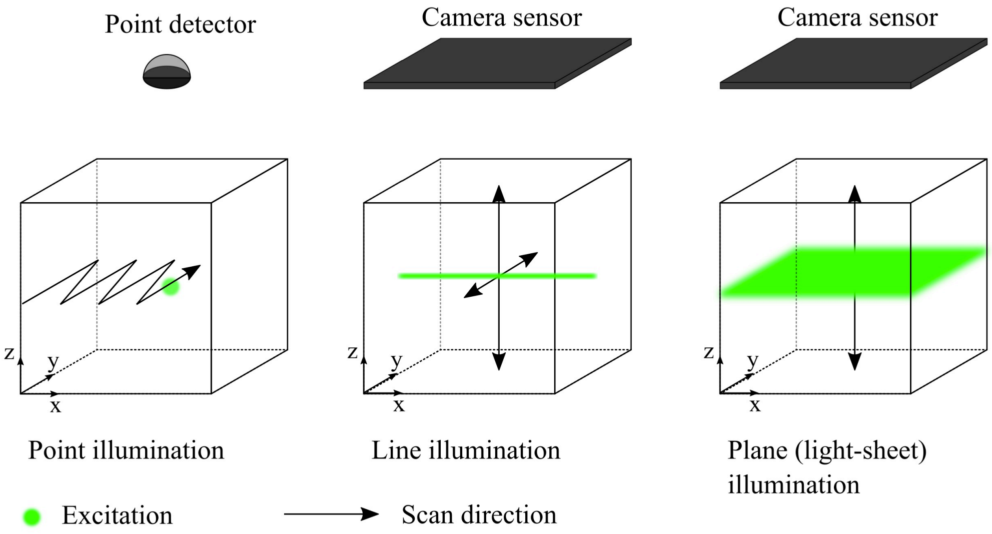

Imperial College London

Light-field Microscopy

Light-Field Microscopy (LFM) is a high-speed imaging technique that uses a simple modification of a standard microscope to capture a 3D image of an entire volume in a single camera snapshot

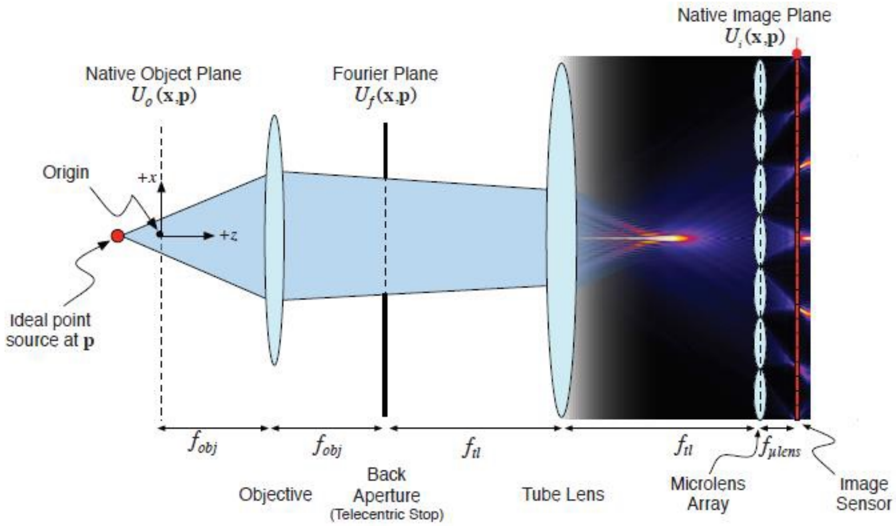

Imperial College London

Light-field Microscopy and EPI

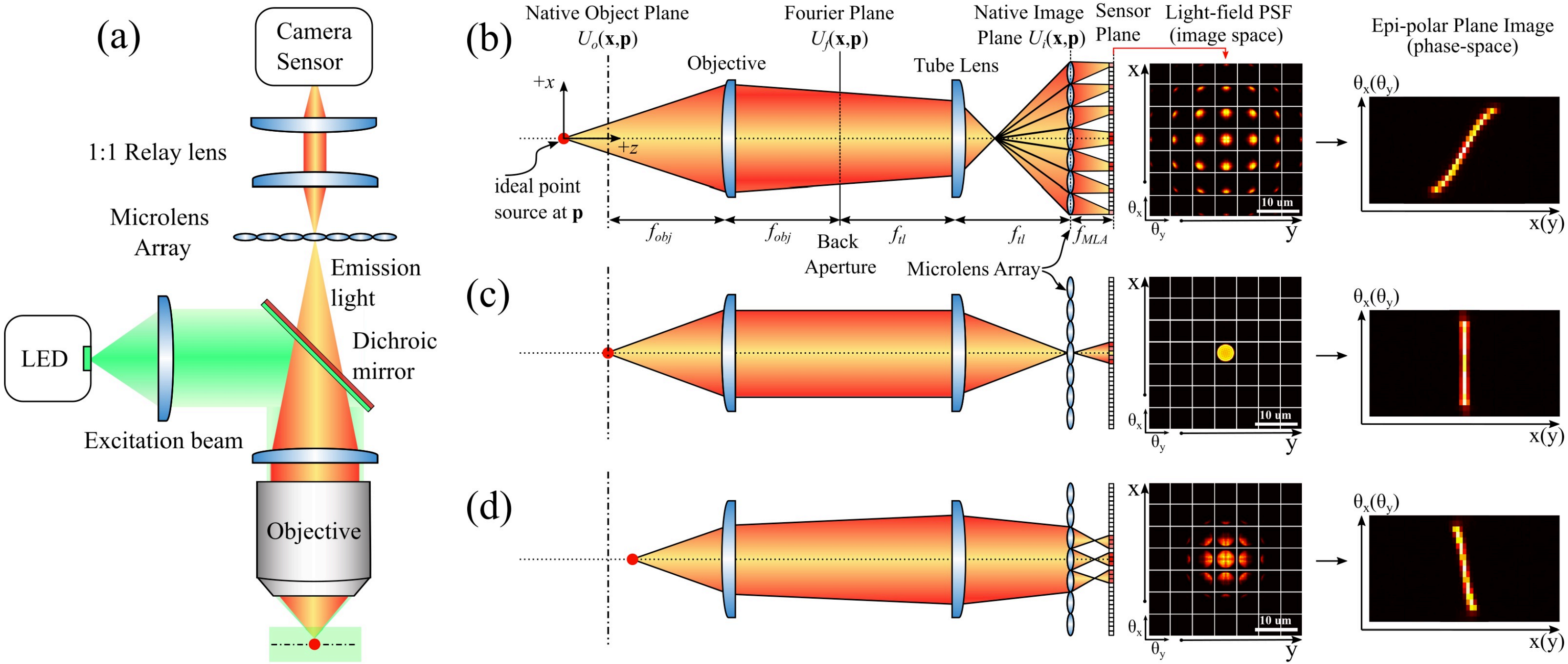

Imperial College London

The Light Field

- First introduced in [LevoyH96]
- Light rays are characterized by their intersection with the camera plane and the image plane
- 4D parameterization of the lightfield

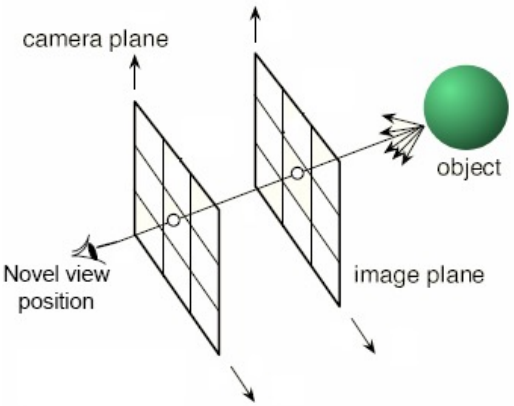

Imperial College London

IBR Results on the Lightfield

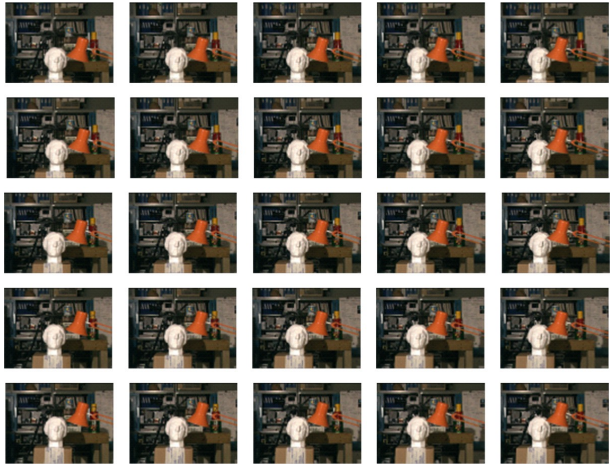

Pearson et al. IEEE TIP 2013

Light-field Microscopy and Illumination Strategies

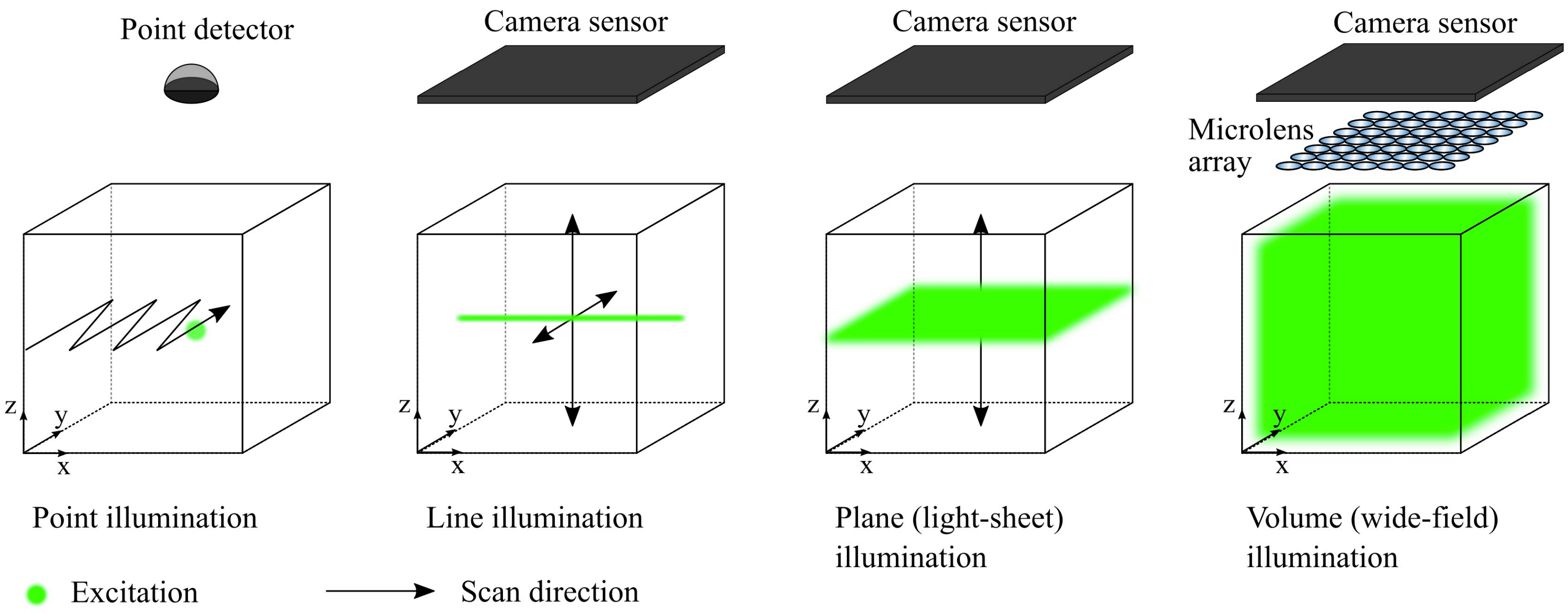

Imperial College London

Real Lightfield Images and EPIs

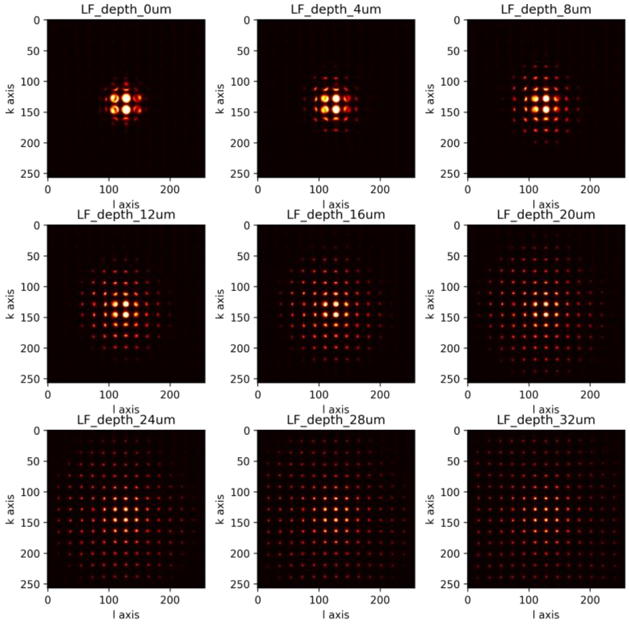

Real LFM for a bead in different depths ranging from 0 to 32 um

Sub-aperture images along vertical and horizontal directions

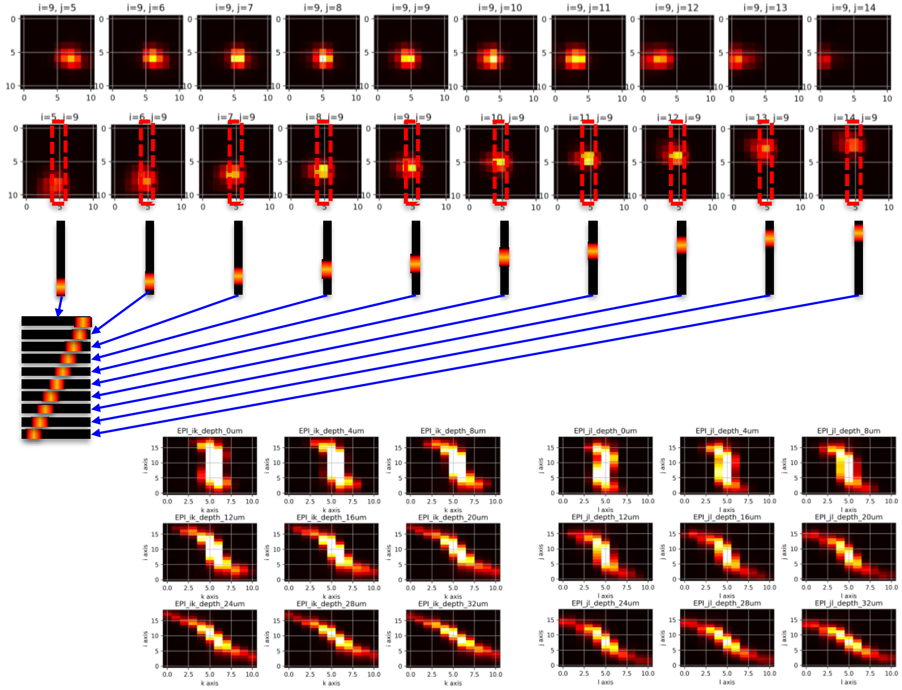

EPIs from real LFM data. i-k direction (left) and j-l direction (right)

Imperial College London

Neuron Localization Approach

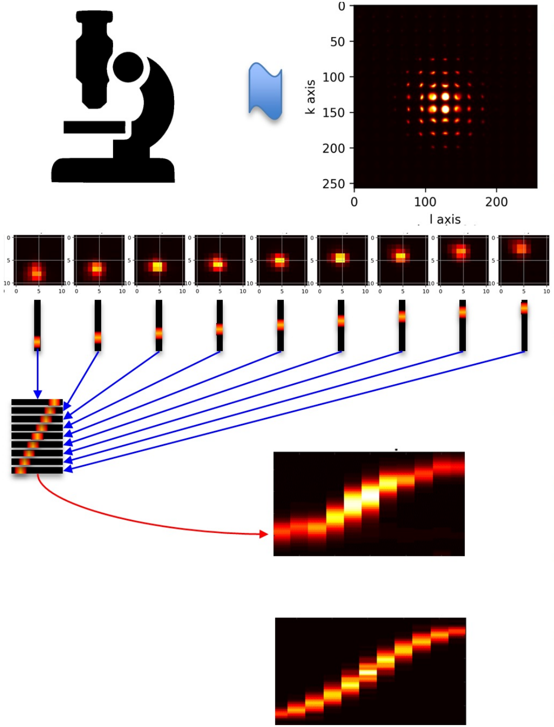

Real LFM → sub-aperture images → EPIs → Convolutional sparse coding → matching EPI atoms

Simulated LFM → sub-aperture images → EPI dictionary → Convolutional sparse coding → Detected location

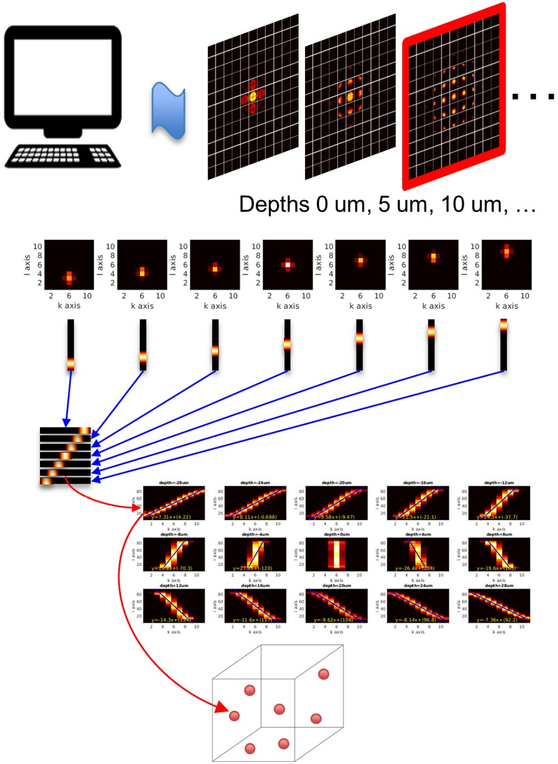

Imperial College London

Dictionary of EPI from Simulated Lightfield Microscope

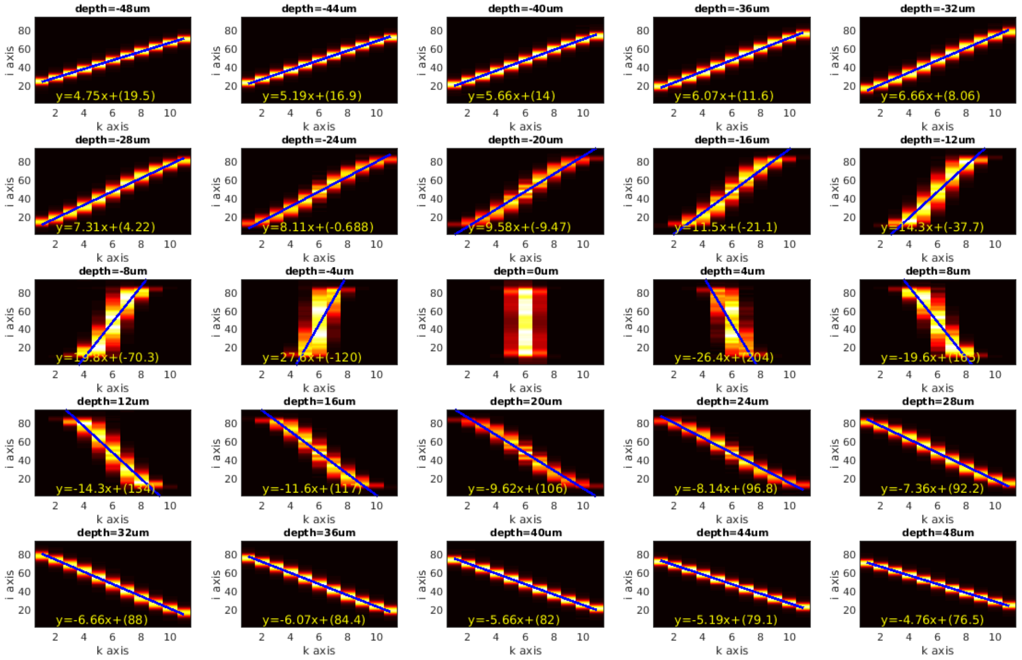

Simulated EPI dictionary. Each atom corresponds to a specific depth

Imperial College London

Convolutional Sparse Coding via ADMM

We develop a convolutional sparse coding algorithm to decompose the input EPI into latent factors to estimate depth and spatial locations.

Objective in image domain:

$$\min_{\mathbf{z}} \quad \frac{1}{2}\|\mathbf{Y} - \sum_{m=1}^{M} \mathbf{d}_m * \mathbf{z}_m\|_2^2 + \beta \sum_{m=1}^{M} \|\mathbf{z}_m\|_1$$

Objective in Fourier domain:

$$\min_{\mathbf{z}_m} \quad \frac{1}{2}\|\hat{\mathbf{Y}} - \sum_{m=1}^{M} \hat{\mathbf{d}}_m \odot \hat{\mathbf{z}}_m\}\|_2^2 + \beta \sum_{m=1}^{M} \|\mathbf{z}_m\|_1$$

Objective in matrix format:

$$\min_{\mathbf{Z}} \quad \frac{1}{2}\|\hat{\mathbf{Y}} - \hat{\mathbf{D}}\hat{\mathbf{Z}}\|_2^2 + \beta \|\mathbf{Z}\|_1$$

Lagrangian

$$\mathcal{L}(\mathbf{Z}, \mathbf{T}, \boldsymbol{\gamma}) = \frac{1}{2}\|\mathbf{Y} - \mathbf{D}\mathbf{Z}\|_2^2 + \beta\|\mathbf{T}\|_1 + \boldsymbol{\gamma}^\top(\mathbf{Z} - \mathbf{T}) + \frac{\mu}{2}\|\mathbf{Z} - \mathbf{T}\|_2^2$$

ADMM algorithm for solving CSC

$$\begin{aligned}
\mathbf{Z}^{(i+1)} &= \arg\min_{\mathbf{Z}} \mathcal{L}(\mathbf{Z}, \mathbf{T}^{(i)}, \boldsymbol{\gamma}^{(i)}) \\
&= \mathcal{F}^{-1}\{(\hat{\mathbf{D}}^\top\hat{\mathbf{D}} + \mu\mathbf{I})^{-1}(\hat{\mathbf{D}}^\top\hat{\mathbf{Y}} - \hat{\boldsymbol{\gamma}} + \mu\hat{\mathbf{T}}^{(i)})\} \\
\mathbf{T}^{(i+1)} &= \arg\min_{\mathbf{T}} \mathcal{L}(\mathbf{Z}^{(i+1)}, \mathbf{T}, \boldsymbol{\gamma}^{(i)}) \\
&= \mathbf{S}_{\beta/\mu}(\mathbf{Z}^{(i+1)} + \boldsymbol{\gamma}^{(i)}/\mu) \\
\boldsymbol{\gamma}^{(i+1)} &= \arg\min_{\boldsymbol{\gamma}} \mathcal{L}(\mathbf{Z}^{(i+1)}, \mathbf{T}^{(i+1)}, \boldsymbol{\gamma}) \\
&= \boldsymbol{\gamma}^{(i)} + \mu(\mathbf{Z}^{(i+1)} - \mathbf{T}^{(i+1)})
\end{aligned}$$

Imperial College London

Location Estimation Algorithm

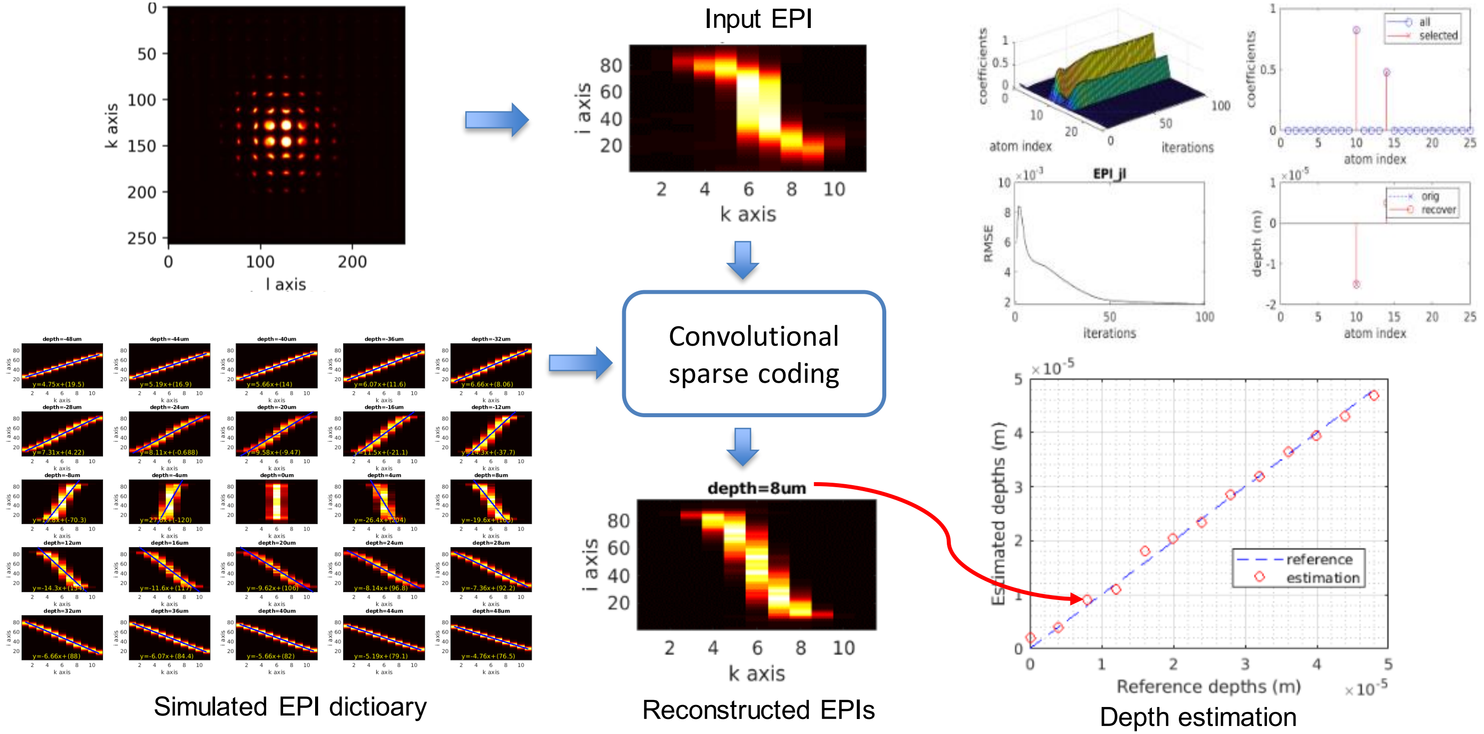

Imperial College London

Numerical Results

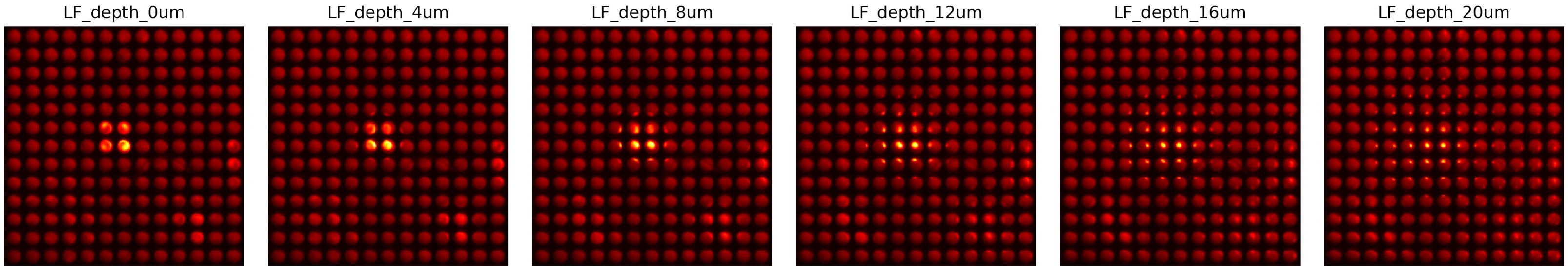

(a) Raw LFM data for a neuronal cell at different depths away from the focal plane.

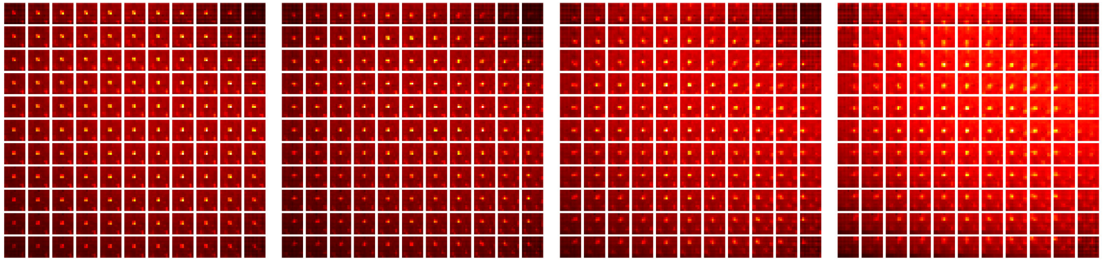

(b) Sub-aperture image arrays for depth 0, 12, 24 and 36 µm, respectively.

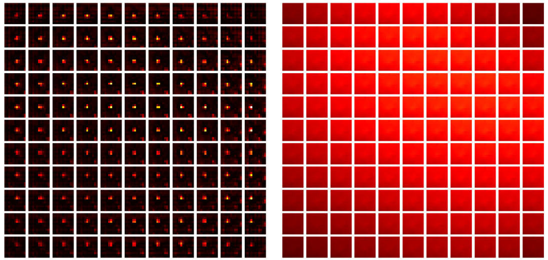

(c) Foreground and Background at depth 12 µm

Numerical Results

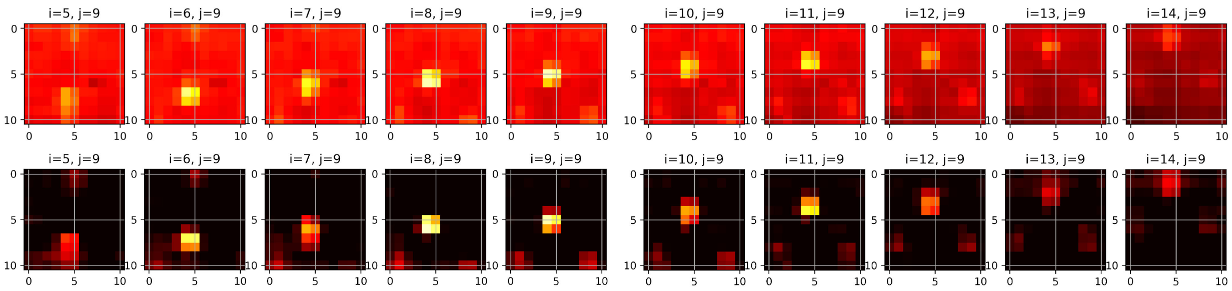

(d) The central column of the sub-aperture image array at depth 36 μm. View changes from down to up. Above: with background. Below: background is removed.

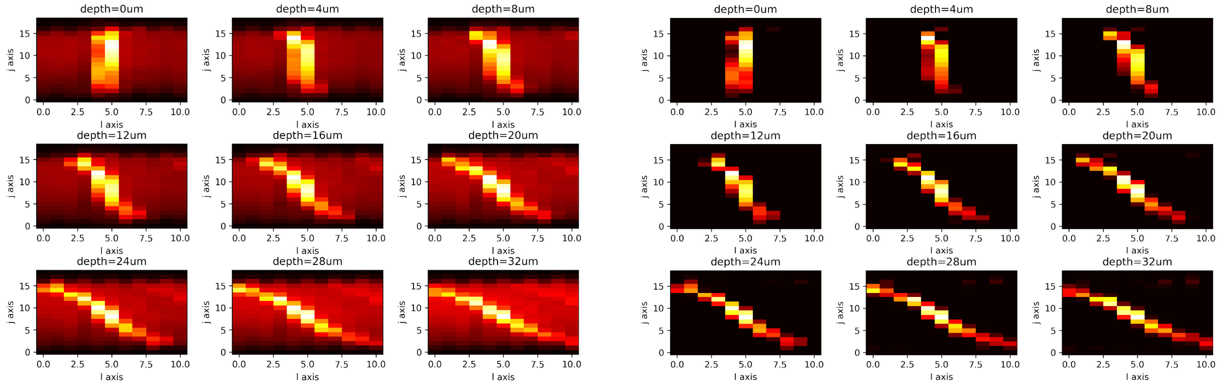

(e) Constructed EPIs in the $j-l$ space.

Purified EPIs in the $j-l$ space without background.

Imperial College London

Numerical Results

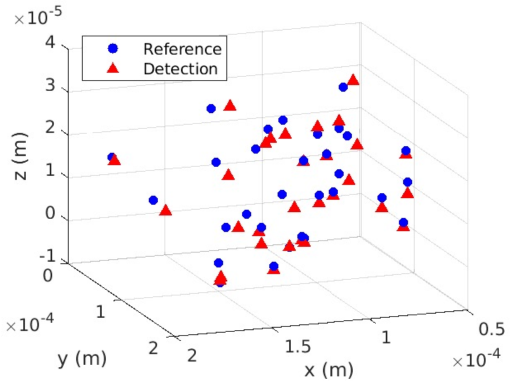

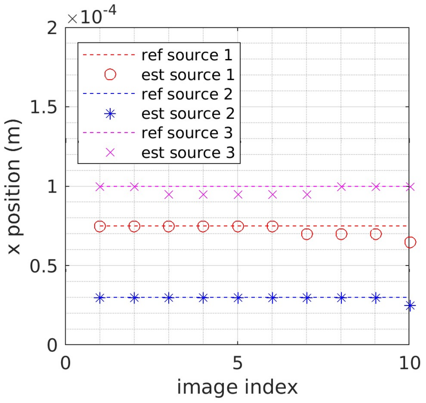

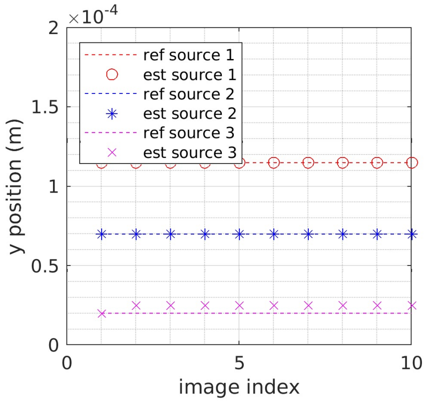

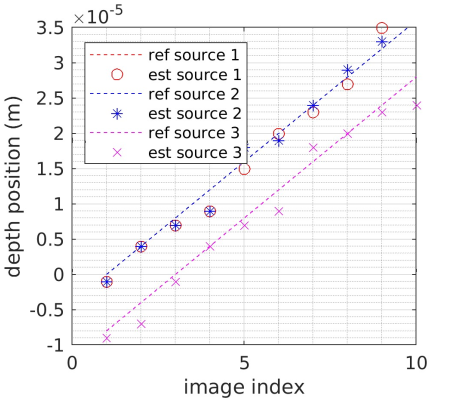

On-going work – CISTA for localization

- The convolutional sparse model leads naturally to an iterative optimization strategy (ISTA) that can be unfolded
- Training based on synthetic data obtained using the Broxton forward model

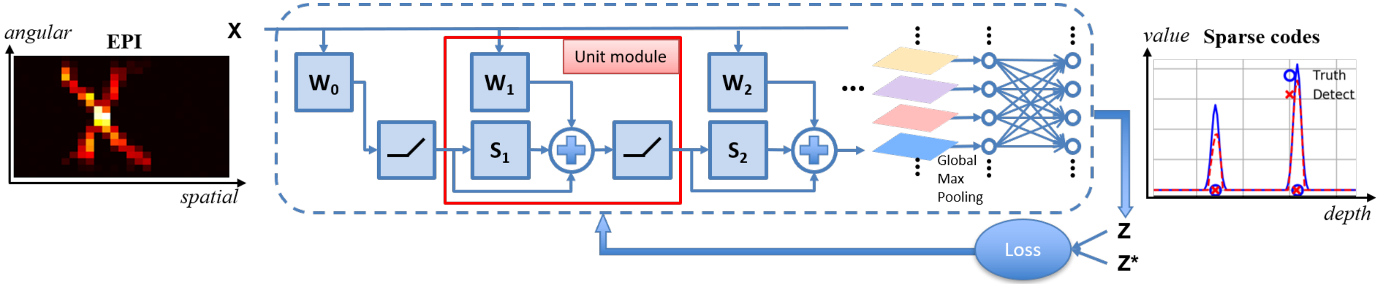

Imperial College London

On-going work – CISTA for localization

(a) Localization performance of phase-space method [6, 8]. RMSE for x, y, z position detection is 4.05, 5.48, 3.41 μm, respectively.

(b) Localization performance of CSC approach [9]. RMSE for x, y, z position detection is 1.78, 2.94, 1.14 μm, respectively.

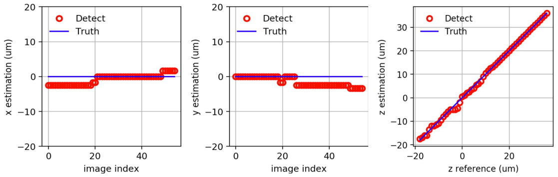

(c) Localization performance of the proposed CISTA-net. RMSE for x, y, z position detection is 1.60, 1.98, 0.82 μm, respectively.

Imperial College London

Conclusions

- Why Computational Imaging?
  - It is fun 🙂
  - It is inter-disciplinary
  - It is the right way to handle ‘big data’: joint sensing, representation, analysis and inference

Thank you!

Imperial College London

References

On Art Investigation

- S. Yan, J.-J. Huang, N. Daly, C. Higgitt, and P. L. Dragotti, “When de Prony Met Leonardo: An Automatic Algorithm for Chemical Element Extraction in Macro X-ray Fluorescence Data”, IEEE Transactions on Computational Imaging, vol.7, 2021.

On Light-Field Microscopy and Neuroscience

- P. Song P, H. Verinaz Jadan, C. Howe, A. Foust and P.L. Dragotti, Light-Field Microscopy for optical imaging of neuronal activity: when model-based methods meet data-driven approaches, IEEE Signal Processing Magazine, to appear in March 2022, http://arxiv.org/abs/2110.13142

- P. Song P, H. Verinaz Jadan, C. Howe, P. Quicke, A. Foust and P.L. Dragotti, 3D localization for light-field microscopy via convolutional sparse coding on epipolar images, IEEE Transactions on Computational Imaging, Vol:6, pages:1017-1032, 2020.